ELSEVIER

Chemical Engineering Journal 144 (2008) 391–399

Chemical Engineering Journal

www.elsevier.com/locate/cej

Cyanobacterial biosorption of Cr(VI): Application of two parameter and Bohart Adams models for batch and column studies

Bala Kiran, Anubha Kaushik *

Department of Environmental Science and Engineering, Guru Jambheshwar University of Science & Technology, Hisar 125 001, India

Received 25 February 2007; received in revised form 4 February 2008; accepted 6 February 2008

Abstract

The present investigation was aimed at analyzing the potential utility of *Lyngbya putealis* HH-15, an indigenous cyanobacterium isolated from a metal contaminated site as a biosorbent of Cr(VI) from aqueous solutions using static and dynamic mode studies. Surface adsorption of the metal at specific binding sites on the algal biosorbent was confirmed through scanning electron microscopy (SEM) and Fourier transform infrared spectroscopy (FTIR) spectral analysis. Kinetic model was applied to study the adsorption process. Intraparticle diffusion plot of the data indicated the involvement of both surface sorption and intraparticle diffusion. Six two-parameter equations (Langmuir, Freundlich, Temkin, Flory–Huggins, Dubinin–Radushkevich, D–R and Brunauer, Emmer and Teller, BET isotherms) were applied to model the equilibrium sorption data on both free and immobilized form of the cyanobacterial biosorbent. In continuous flow column experiments effects of bed height (5–10 cm), flow rate (1–3 mL/min), and initial metal ion concentration (5–20 mg/L) on breakthrough time and adsorption capacity of the immobilized biosorbent were studied. The data generated was developed into a model based on empirical relationship of the Bohart–Adams model. The column regeneration studies were also performed using 0.1 M HCl for five cycles. The high chromium removal ability and regeneration efficiency of this biosorbent suggest its applicability in industrial processes and data generated would help in further upscaling of the adsorption process.

Keywords: Chromium; Cyanobacteria; Adsorption isotherms; Sorption–desorption

1. Introduction

Passive removal of heavy metals from aqueous solution using various types of biosorbents including bacteria, fungi, algae and yeast have been investigated extensively in the recent years [1,2]. Amongst these, cyanobacterial biosorbents are found to be more promising due to their simple nutrient requirements, larger biomass production and generally non-toxic nature. Their cell wall along with the outer mucilagenous sheath comprises an array of ligands with several functional groups providing sites for binding various metallic ions. Use of dry powdered form of algal biomass for biosorption however, has limitations for column applications due to low strength, small particle size and problem of separation from wastewater after use [3]. A more effective technique is immobilization in a polymeric matrix like gel involving formation of beads, which provide mechanical strength and rigidity to the system [4].

Most of the research was earlier restricted to batch studies, providing fundamental information on applicability of various biosorbents for removal of metals. However, it had limited use in column studies where sufficient contact time was not available for attainment of equilibrium [5].

In the present study, the potential of *Lyngbya putealis* HH-15 [Synonym. *Phormidium putealis*; [6], a cyanobacterium isolated from a metal contaminated soil has been investigated in free and immobilized forms in batch mode for the removal of chromium(VI) from aqueous solution applying various two-parameter isotherms and kinetic model to the data along with surface characterization of the biosorbent. Efficiency of the immobilized biosorbent for biosorption, desorption and regeneration have also been studied in column mode and modeled to assess its practical applicability.

* Corresponding author. Tel.: +91 1662 263164; fax: +91 1662 277942.
E-mail address: aks_10@yahoo.com (A. Kaushik).

1385-8947/$ – see front matter © 2008 Elsevier B.V. All rights reserved.
doi:10.1016/j.cej.2008.02.003

2. Materials and methods

2.1. Cyanobacterial isolation and culture

2.1.1. Lyngbya putealis

HH-15 was isolated from metal contaminated soil collected from within the premises of an electroplating industry in Haryana, India (28°55′N 76°43′E), which is a semi-arid subtropical region. The soil in the region shows moderate organic carbon and high concentration of soluble salts that accumulated in the upper profile due to high solar intensity, high evaporation rates and low annual rainfall (475 mm). The soil has a water holding capacity of 38% and chromium concentration ranges from 2 to 8 mg/kg soil. The cyanobacterial species are exposed to the metal concentration in the soil for about 30 years. Pure culture of the cyanobacterium was obtained by streaking on basal agar medium at pH 8.5 using standard isolation and culturing techniques on nitrogen supplemented BG-11 medium [7]. The algal cultures were maintained at a light intensity of 3000 lux using cool fluorescent tubes at 28 ± 3 °C in a culture room.

2.2. Fourier transform infrared (FTIR) spectroscopy and scanning electron microscopy (SEM)

FTIR spectroscopy was used to predict the vibrational frequency changes in the algal biosorbent. The spectra were obtained by JASCO FTIR-660 PLUS spectrometer within the range 500–4500 cm^{-1} using a KBr window. The surface morphology of the dry adsorbent before and after chromium loading was visualized by SEM (Philips PSEM 515).

2.3. Preparation of biosorbent

Dry cyanobacterial biosorbent: 14-day old algal cultures were harvested and the algal biomass was washed with distilled water and oven dried at 70 °C for 24 h before use in powdered form.

Immobilized cyanobacterial biosorbent: 0.1 g dry weight of the cyanobacterial biomass was suspended in 5 mL of double distilled water, mixed with 4% sodium alginate solution (w/v) and dropped into 0.5 M calcium chloride solution using a syringe to form algal beads (3.0 ± 0.1 mm diameter). The beads were kept overnight at 4 °C in $CaCl_2$ (0.5 M) for completing the process of gelation. The beads were repeatedly washed with double-distilled water and stored at 4 °C in distilled water prior to use as the biosorbent [4]. Blank alginate beads were also prepared using similar procedure, but without the alga.

2.4. Batch adsorption studies

A stock solution of the aqueous adsorbate, Cr(VI) (1000 mg/L) was prepared using potassium dichromate (AR grade) and desired concentrations of the metal were obtained by further dilutions. Batch studies were performed to determine the equilibrium time required for adsorption of Cr(VI) on the algal bisorbents. Erlenmeyer flasks containing 100 mL of the metal solution at initial pH 2 having biosorbent (0.1 g algal dry weight) were shaken on an illuminated orbital shaker (Orbitek LT-IL) with fluorescent light at 120 rpm at 25 °C. Samples were withdrawn at fixed time intervals from the flasks and analyzed spectrophotometrically for residual metal ion concentration in the aqueous solution. Equilibrium studies were performed using different initial metal ion concentrations (10–100 mg/L) with 0.1 g biosorbent concentration at pH 2 and temperature of 25 °C. pH of the aqueous metal solution was adjusted using 0.1 M HCl. All the experiments were performed in triplicates and their mean values are reported here.

Amount of metal adsorbed, q_e (mg/g of dry weight of alga) was determined using the equation

$$q_e(\mathrm{mg/g}) = \frac{V(C_0 - C_e)}{m} \quad (1)$$

where C_0 is initial metal concentration (mg/L), C_e the equilibrium metal concentration (mg/L), V the volume of metal solution (L) and m is the mass of dry alga (g).

Percent removal was calculated as the ratio of difference in initial and final metal concentration ($C_0 - C_e$) to initial chromium concentration (C_0):

$$R(\%) = \frac{C_0 - C_e}{C_0} \times 100 \quad (2)$$

2.5. Column studies

Immobilized alga in the form of alginate beads was used for column studies. Glass column (2 cm i.d.) was taken with glass wool at the bottom and glass beads at the top (2 cm layer) to provide a uniform inlet flow to column. A known quantity of biosorbent was placed to obtain the desired bed height in the column. Chromium solution of known concentration (pH 2) was passed through the column and samples were collected at regular time intervals. The operation was conducted in down flow mode. All the experiments were conducted at room temperature.

After exhaustion of the column, the biosorbent was regenerated using 0.1 M HCl at a flow rate of 2 mL/min. After desorption, column bed was washed with distilled water till pH of outlet solution reached 7.0. The bed was reused for next cycle and the sorption–desorption study was carried out for five cycles.

2.6. Metal analysis

Concentration of Cr(VI) ions in the synthetic solution was analyzed using a Systronics Spectrophotometer-106 at 540 nm using 1,5-diphenyl carbazide reagent in acid solution as complexing agent for Cr(VI) [8].

3. Results and discussion

3.1. Biosorbent surface studies

Fourier transform infrared (FTIR) was used to determine the changes in vibration frequency in the functional groups of the biosorbent due to metal sorption. The spectra of the dry alga were measured within a range of 500–4500 cm^{-1} wave number. Surface morphology of the biosorbent with and without metal loading was studied using scanning electron microscope.

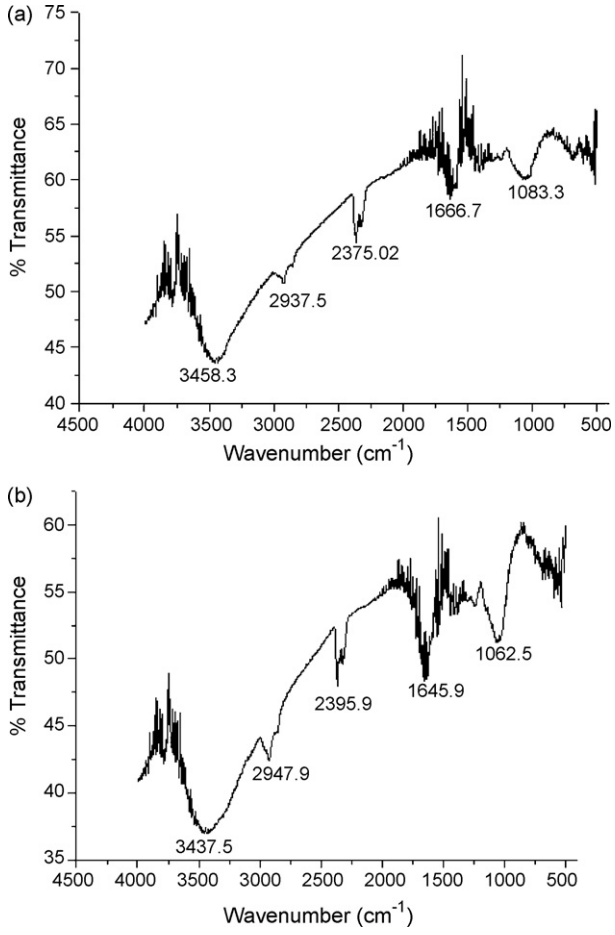

Fig. 1. FTIR spectra of dry algal adsorbent (a) before and (b) after metal adsorption.

A perusal of the FTIR spectra of control and metal loaded cyanobacterial biosorbent *L. putealis* are shown in Fig. 1. The FTIR spectrum reveals complex nature of the biosorbent as evidenced by the presence of a large number of peaks. Adsorption peak around 3458.3 cm^{-1} indicates the existence of –NH, which shifts to 3437.5 cm^{-1} after chromium loading indicating binding of the metal to this functional group. The peak at about 2937.5 cm^{-1} shifts to 2947.9 cm^{-1} after metal loading indicates the involvement of –CH stretch. Spectral bands of the biosorbent shifting from 2375.02 to 2395.9 cm^{-1} before and after metal treatment also suggests involvement of –C to N. The peak at 1666.7 cm^{-1} indicated C=C stretching that shift to 1645.9cm^{-1} and the adsorption peak at 1083.3 cm^{-1} due to $–OCH_3$ group which showed a shift to lower frequency of 1062.5cm^{-1} after metal loading indicate the involvement of these functional groups in metal binding onto the cyanobactrial biosorbent. Distinct variations caused in the surface microstructure of the adsorbent after metal adsorption are further illustrated in scanning electron micrographs of the cyanobacterial biosorbent before and after chromium loading (Fig. 2).

3.2. Sorption mechanism

In order to interpret the experimental data, prediction of rate limiting step is important. In a solid–liquid sorption process, solute transfer may take place by boundary layer diffusion or intraparticle diffusion or both. Vadivelan and Kumar [9] describe three consecutive steps in sorption dynamics as transport through liquid film to exterior surface, solute diffusion into the pores of the adsorbent and a rapid step of sorption of solute on the interior surfaces of the pores. The overall sorption is determined by the rate limiting steps of film diffusion or pore diffusion. For understanding the sorption of chromium onto the biosorbent kinetic model was applied. A common method used for the identification of mechanism involved in the sorption process is by fitting the data into intraparticle diffusion plot. A plot of q_t versus $t^{0.5}$ has often been reported to represent multilinearity characterizing two or more steps involved in the sorption process [10]. The mathematical expression for intraparticle diffusion model is

$$q_t = K_p t^{0.5} \quad (3)$$

where K_p (mg/g $min^{0.5}$) is the intraparticle diffusion rate constant and its value can be obtained from the slope of the plot q (mg/g) versus $t^{0.5}$ ($min^{0.5}$).

Fig. 3 shows the plot of q_e versus $t^{0.5}$ for the chromium sorption onto the immobilized and dry powdered algal sorbent. It is observed that the curve shows two phases for algal beads. The

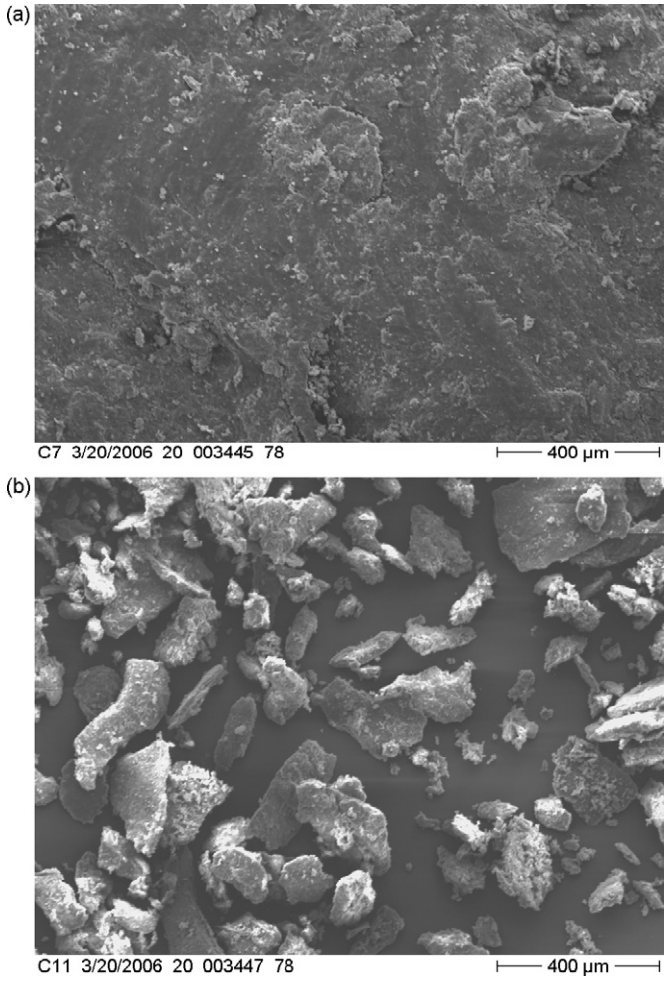

Fig. 2. Scanning electron micrograph (SEM) of dry algal adsorbent (a) before and (b) after metal adsorption.

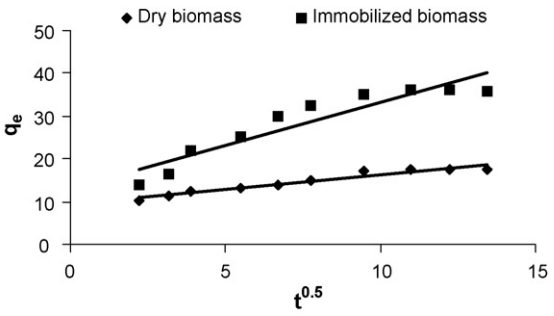

Fig. 3. Intraparticle diffusion model for the sorption of chromium(VI) onto dry and immobilized algal biomass.

curve is comparatively linear for dry biomass. However, it does not pass through the origin indicating that intraparticle diffusion is not the only mechanism involved in sorption process. The two phases in the plot suggest that there is involvement of both surface sorption and intraparticle diffusion. The initial curved part and second linear portion indicate boundary layer effect and intraparticle diffusion, respectively. The slope of the second linear portion can be explained by K_p (mg/g min$^{0.5}$). The values for K_p are 0.67 and 2.03 mg/g min$^{0.5}$ for dry biomass and algal beads, respectively. The intercept of the plot indicates boundary layer effect. Higher value of intercept for beads (12.97) shows greater contribution of surface sorption in the rate-limiting step of immobilized form as compared to that in free form.

3.3. Adsorption equilibrium

Adsorption equilibrium data of the biosorbents was explained with the following isotherms.

Langmuir isotherm assuming that there are finite numbers of binding sites distributed homogeneously over the surface of the adsorbent, can be represented as

$$q_e = \frac{Q_0 b C_e}{1 + bC_e} \quad (4)$$

where Q_0 (mg/g) and b (L/mg) are Langmuir constants showing the adsorption capacity and energy of adsorption, respectively [11]. Langmuir isotherm showed linear plots and values of Langmuir constants (Q_0 and b) were calculated from the slope and intercept of the plots. Adsorption capacity was very high (111.11 mg/g) for dry algal biomass (Table 1).

Furthermore the favorability of adsorption was tested using a dimensionless constant called separation factor (R_L), which is an essential feature of Langmuir isotherm:

$$R_L = \frac{1}{1 + bC_0} \quad (5)$$

The values of R_L for the biosorbents, free (0.11); immobilized (0.28) ranging between 0 and 1 confirm feasibility of chromium sorption onto these biosorbents.

Freundlich isotherm applied to study the adsorption behavior assumes heterogeneous surface of the adsorbent and linearized form of the model is as follows:

Table 1
Isotherm constants of two parameter models for chromium(VI) biosorption onto dry and immobilized algal biomass

Isotherm	Dry algal biomass	Immobilized algal biomass
Langmuir		
Q_0 (mg/g)	111.11	7.72
b (L/mg)	0.167	0.053
R^2	0.8939	0.6932
Freundlich		
K_f (mg/g)	15.98	6.42
N	1.49	1.984
R^2	0.821	0.8569
Temkin		
a (L/g)	1.83	6.08
b (kJ/mol)	0.101	0.052
R^2	0.945	0.9697
Flory–Huggins		
K_{FH}	435.8	14.77
n_{FH}	0.901	1.31
ΔG° (kJ/mol)	−15.03	−6.66
R^2	0.2146	0.6439
Dubinin–Radushkevich		
q_D (mg/g)	101.9	224.5
B_D (mol^2/kJ^2)	0.26	2.19
E (kJ^2/mol^2)	1.39	0.48
R^2	0.9691	0.9518
BET		
q_{max} (mg/g)	111.11	18.83
B (L/mg)	2.25×10^4	0.59×10^4
R^2	0.894	0.3013

$$\text{Log}\, q_e = \text{Log}\, K_f + \frac{1}{n}(\text{Log}\, C_e) \quad (6)$$

where K_f is Freundlich constant indicating adsorbent capacity (mg/g dry weight), n Freundlich exponent known as adsorbent intensity [12]. Linear plot of Log q_e versus Log C_e shows the applicability of this isotherm for both the systems. The values of K_f and n along with R^2 calculated from the plots are given in Table 1. The high values of K_f and n confirm high feasibility of Cr(VI) adsorption on the algal surface from metal containing wastewater.

The comparison of Langmuir and Freundlich constants (Table 1) obtained for these dry and immobilized cyanobacterial biosorbents shows that the value of both Q_0 (111.1 and 7.72 mg/g for dry and immobilized respectively) and K_f (15.98 and 6.42 mg/g for dry and immobilized, respectively) is higher for dry as compared to immobilized [13].

Temkin isotherm assumes that fall in heat of sorption is linear rather than logarithmic, as given in Freundlich equation [14]. Due to sorbate/sorbent interactions the heat of sorption of all the molecules in layer would decrease linearly with coverage [15]. This isotherm has been applied in following form:

$$q_e = \frac{RT}{b} \ln(aC_e) \quad (7)$$

where b is the Temkin constant related to heat of sorption (kJ/mol), R the gas constant (0.0083 kJ/mol K), a the Temkin isotherm constant (L/g) and T is the absolute temperature (K).

The curve was plotted between q_e and $\ln C_e$. Values of both constants a and b were calculated as presented in Table 1. It has been observed that value of Temkin sorption potential, a, is quite high (6.077 L/g) for beads and also the value of R^2 is higher for beads (0.9697) as compared to free alga. Typical bonding energy range for ion-exchange mechanism is reported to be 8–16 kJ/mol [16]. It is observed that up to −20 kJ/mol is surface indicative of physisorption process due to electrostatic interaction between charged molecules whereas more negative than −40 kJ/mol involves chemisorption [17]. Low values in the present study (0.05–0.10 kJ/mol) indicate that interactions between the sorbate and sorbent are neither purely through ion-exchange nor purely through physisorption.

Flory–Huggins isotherm applied to study the degree of surface coverage [18] is given by the equation

$$\mathrm{Log}\frac{\theta}{C_0} = \mathrm{Log}\, K_{FH} + n_{FH}\,\mathrm{Log}(1-\theta) \tag{8}$$

where K_{FH} is Flory–Huggins model equilibrium constant; n_{FH} is the Flory–Huggins model exponent; $\theta = ((1 - C_e)/C_0)$ is degree of surface coverage. The isotherm showed linear plots for both the adsorbents. Values of (K_{FH} and n_{FH}) calculated from the slope and intercept of the plots are given in Table 1. Suitability of the model to immobilized algal beads is indicated by high value of R^2 (0.6439) whereas the free form showed little applicability due to low regression coefficient.

K_{FH} was further used to calculate the Gibbs free energy of spontaneity (ΔG°):

$$\Delta G^\circ = -RT \ln K_{FH} \tag{9}$$

For both the biosorbents ΔG° is negative (Table 1) indicating spontaneous nature and feasibility of chromium biosorption onto these biosorbents supporting an exothermic reaction.

Dubinin–Radushkevich isotherm assumes that characteristic sorption curve is related to the porous structure of the sorbent [19]:

$$q_e = q_D \exp(-B_D E_D^2) \tag{10}$$

$$E_D = RT \ln\left(1 + \frac{1}{C_e}\right) \tag{11}$$

where q_D (mg/g) and B_D (mol^2/kJ^2) are the Dubinin–Radushkevich model constants; E_D is the Polanyi potential.

The mean energy of sorption can be calculated as follows:

$$E = \frac{1}{\sqrt{2B_D}} \tag{12}$$

Values of both the constants along with R^2 (Table 1) are higher for beads showing better fitness of the isotherm. The energy values for both the biosorbents (free and immobilized) are very low (1.39 and 0.48 kJ^2/mol^2, respectively) indicating weak metal–sorbents interaction in consonance with the predictions of Temkin isotherm.

Brunauer, Emmer and Teller (BET) model developed for multimolecular layers is an extension of Langmuir model [20] assumes that first surface layer adsorption occurs with energy comparable to heat of monolayer sorption and subsequent layers have equal energies, explained as follows:

$$q_e = \frac{Bq_{max}C_e}{(C_e - C_s)[1 + (B-1)(C_e/C_s)]} \tag{13}$$

where C_s is the saturation concentration of solute (mg/L) and B is a constant related to energy of adsorption. Curve was plotted for both the biosorbents and the values of q_{max} and B calculated from the intercept and slope are given in Table 1. Higher coefficient of determination for free cyanobacterial biomass shows its greater applicability of this model-indicating multilayer adsorption process for this biosorbent and higher value of R^2 for Langmuir isotherm suggests that Langmuir equation applies to each layer of multilayer [11].

3.4. Regression coefficient of determination

To find out greater suitability of data amongst various isotherms used for the two biosorbents, two-way analysis of variance (ANOVA) without replication was applied to R^2 values. High average R^2 value suggests that D–R provides a better model for sorption and dry biosorbent exhibits a better fitness to six isotherm models. However, variations in determination coefficients due to different isotherms ($F = 1.58$, d.f. = 5, $P < 0.05$) and biosorbents ($F = 0.15$, d.f. = 1, $P < 0.05$) were not statistically significant indicating every model to be important in its own capacity and adsorptive capacity of both biosorbents was good.

Comparison of the present biosorbents with other biosorbents reported in literature shows that maximum adsorption capacity (Q_0) for *L. putealis* HH-15 (111.11 mg/g) is more as compared to *Dunaliella* sp. (102.5–111.0 mg/g) [21], *Chlorella vulgaris* (79.3 mg/g) [22] and *Scendesmus obliquus* (58.8 mg/g) [23] indicating its greater effectivity for chromium removal.

3.5. Column studies

3.5.1. Adsorption capacity of column

As the adsorbate solution moves, adsorption zone also starts moving. After some time effluent concentration starts rising, this is termed as break point. So break through time (t_b) is defined as the time required to reach a specific break through concentration (50% of initial concentration C_i).

Break through capacity calculated according to Treybal [24] is expressed as mg of chromium(VI) adsorbed per gm of adsorbent.

$$\text{Break through capacity } (Q_{50\%}) = \frac{\text{break through time (at 50\%)} \times \text{flow rate} \times \text{initial Cr conc.}}{\text{mass of adsorbent in the bed}}$$

Chromium adsorption capacity in column calculated for varying bed height, initial chromium concentration and flow rate is presented in Table 2. It was found to be 0.7 mg/g for a bed height of 10 cm, flow rate of 1 mL/min and metal concentration of 20 mg/L for 50% break through concentration. It is observed that adsorption capacity is less for column experiments as com-

Table 2
Column adsorption capacity ($Q_{50\%}$) at various operating conditions of flow rate (ml/min), bed height (cm), and inlet concentration (mg/L)

Inlet concentration (mg/L)	Break point (50%) (min)	Flow rate (mL/min)	Bed height (cm)	Adsorption capacity (mg/g)
5	60	1	10	0.30
10	50	1	10	0.50
15	40	1	10	0.60
20	35	1	10	0.70
10	23	2	10	0.46
10	13	3	10	0.39
10	17	1	5	0.34
10	30	1	7.5	0.40

pared to that calculated from batch studies. The reason may be the less stirred property in column mode.

3.5.2. Effect of bed height

Adsorption of metal is dependent on the quantity of sorbent in the column. Break through experiments were conducted at constant metal concentration of 10 mg/L, flow rate of 1 mL/min and varying bed heights of 5, 7.5 and 10 cm and break through curve was plotted between ratio of final (outlet) and initial chromium concentration (C_{out}/C_{in}) and time (min) (Fig. 4). It was observed that break through time increased with increasing bed height which seems attributed to increase in number of binding sites broadening the mass transfer zone. The chromium adsorption capacity was also increased with bed height and was found to be maximum at 10 cm, which was selected as the optimized bed height for further experiments.

3.5.3. Effect of flow rate

Flow rate is an important parameter for evaluating the efficiency of sorbents in continuous treatment process of effluents on pilot or industrial scale. It was studied at constant initial chromium concentration of 10 mg/L and bed height of 10 cm by varying flow rate from 1 to 3 mL/min. Break through curve is shown in Fig. 4. It was observed that break through time decreased from 50 to 13 min when flow rate increase and from 1 to 3 mL/min. This may be due to the increase in speed of adsorption zone at increased flow rate, which resulted in decrease in the time required to reach the specific break through concentration. Flow rate also influenced the chromium adsorption. It was found to be 0.5, 0.46 and 0.39 mg/g for 1, 2, and 3 mL/min, respectively. This may be due to insufficient time for adsorption and diffusion limitations of sorbate on the sorbent in column at higher flow rates.

3.5.4. Effect of initial chromium concentration

Fig. 4 shows the effect of initial chromium concentration on break through curve. Break through time decreased with increasing metal concentration from 5 to 20 mg/L, because with increasing metal concentration, metal loading rate increases resulting in decreased adsorption zone length. The main effect is increase in adsorption capacity with increasing chromium concentration as shown in Table 2.

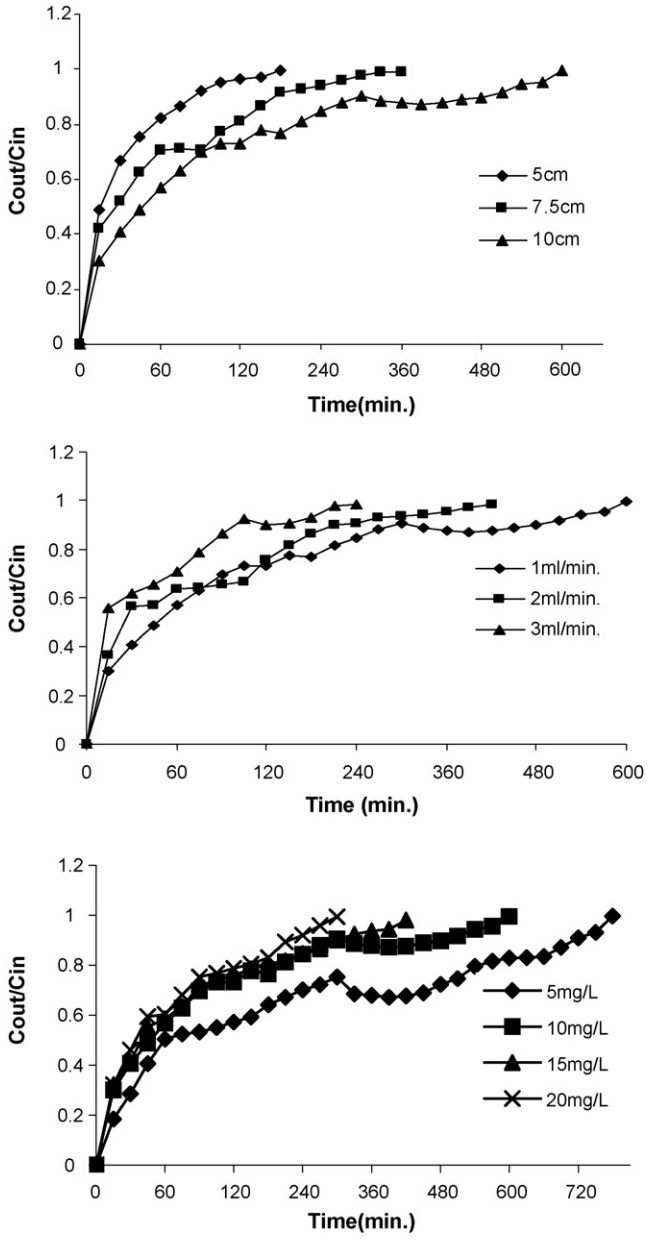

Fig. 4. Breakthrough curve for varying (a) bed height (cm) at flow rate of 1 mL/min and 10 mg/L inlet concentration, (b) flow rate (mL/min) at bed height of 10 cm and 10 mg/L inlet concentration and (c) inlet chromium concentration (mg/L) at bed height of 10 cm and 1 mL/min of flow rate.

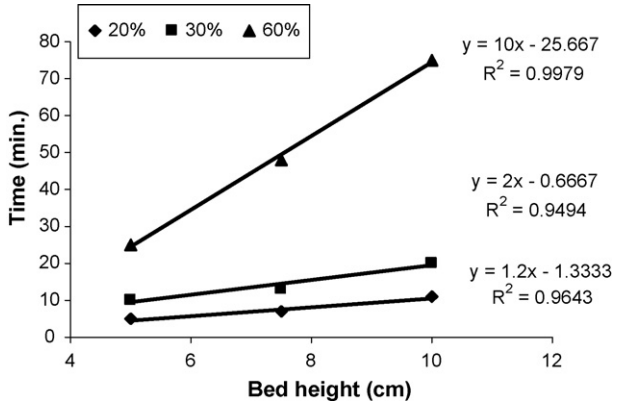

Fig. 5. Bohart–Adams model for 20, 30 and 60% breakthrough at different bed heights and constant inlet concentration (10 mg/L) and flow rate (1 mL/min).

3.5.5. Bohart–Adams model

This is based on the assumption that sorption is a continuous process wherein equilibrium is not attained instantaneously and the rate of sorption is proportional to sorption capacity that still remains on sorbent [25]. This model is based on surface reaction theory [26] and the performance of continuous column can be predicted by the following equation:

$$t = \frac{N_0 Z}{C_i V} - \frac{1}{KC_i} \ln\left(\frac{C_i}{C_b} - 1\right) \quad (14)$$

where C_i is the initial metal ion concentration (mg/L), C_b the breakthrough metal ion concentration (mg/L), t the time to breakpoint (min), N_0 the sorption capacity of biosorbent (mg/L), Z the bed height of column (cm), V the linear velocity (cm/min) and K is the rate constant (L/mg min).

Equation for Bohart–Adam model can be written as

$$t = mx + c \quad (15)$$

where $m = N_0/C_i V$ and $c = 1/KC_i \ln(C_i/(C_b - 1))$.

Under constant experimental conditions (flow rate = 1 mL/min, initial chromium concentration = 10 mg/L), iso-removal lines were plotted between time and bed height as shown in Fig. 5. From the slope and intercept of respective iso-removal line, the adsorption capacity (N_0) and rate constant of adsorption (K), were calculated (Table 3).

Linear equation developed for one metal concentration can also be applied to another concentration as modified:

$$m_{new} = m_{old}\left(\frac{C_i}{C_n}\right) \quad (16)$$

Table 3
Bohart–Adams model constants for the adsorption of chromium(VI) on immobilized adsorbent

Iso-removal percentage	m (min/cm)	c (min)	N_0 (mg/L)	K (L/mg min)	R^2
20	1.2	−1.33	3.82	0.104	0.9643
30	2	−0.67	6.36	0.126	0.9494
60	10	−25.67	31.8	−0.0016	0.9979

$$c_{new} = c_{old}\left(\frac{C_i}{C_n}\right)\left[\frac{\ln(C_n - 1)}{\ln(C_i - 1)}\right] \quad (17)$$

where C_i and C_n are the original and new chromium concentrations.

Similarly slope constant can be calculated for flow rate (V_n):

$$m_{new} = m_{old}\left(\frac{V_o}{V_n}\right) \quad (18)$$

By applying these equations, breakthrough time was found out for new chromium concentration and flow rate (Tables 4 and 5). These were then compared with the observed breakthrough time obtained from experimental results. It is also proved by low standard deviation (Tables 4 and 5). Thus, the developed model can be used for the designing of column over a range of flow rate and metal concentration.

3.5.6. Regeneration of the biosorbent

It is of much importance to reuse the biosorbent for metal removal in industrial applications. Reusability of any biosorbent can be evaluated by its sorption performance in successive sorption/desorption cycles. Immobilized cyanobacterial cells were tested in five cycles using 0.1 M HCl as a desorbing agent at 2 mL/min. The breakthrough time, exhaustion time, breakthrough uptake capacity (mg/g) for all the five cycles is given in Table 6.

Regeneration efficiency (%) was calculated using the equation:

$$RE(\%) = \frac{q_{reg}}{q_{org}} \times 100$$

where q_{reg} is the adsorptive capacity of the regenerated column and q_{org} is the original capacity (mg/g) of the adsorbent. The regeneration efficiency was calculated for all the five cycles and is given in Table 6. It has been observed that RE (%) was found to be 40% after fifth cycle.

Table 4
Predicted breakthrough time (min) using Bohart–Adams constants for a new inlet concentration (mg/L)

Break point (%)	m_{old}	c_{old}	C_i	C_n	C_i/C_n	m_{new}	c_{new}	Bed height (cm)	Predicted time (min)	Observed time (min)	E^*
20	1.2	−1.33	10	5	2	2.4	−1.68	10	22.3	20	0.03
30	2	−0.67	10	5	2	4	−0.85	10	39.2	35	
60	10	−25.7	10	5	2	20	−32.4	10	167.6	160	

* $E = \sum_{J=1}^{N} [(q_e)_{obs} - (q_e)_{predict}]^2 (q_e)_{obs}$.

Table 5
Predicted breakthrough time (min) using Bohart–Adams constants for a new flow rate (mL/min)

Break point (%)	m_{old}	c_{old}	V_o	V_n	V_o/V_n	m_{new}	Bed height (cm)	Predicted time (min)	Observed time (min)	E[a]
20	1.2	−1.33	1	2	0.5	0.6	10	6	7	0.06
30	2	−0.67	1	2	0.5	1	10	10	12	
60	10	−25.7	1	2	0.5	5	10	50	55	

[a] $E = \sum_{J=1}^{N} [(q_e)_{obs} - (q_e)_{predict}]^2 (q_e)_{obs}$.

Table 6
Sorption–desorption parameters for five cycles

Cycle no.	Breakthrough uptake (mg/g)	Breakthrough time (min)	Bed exhaustion time (min)	Regeneration efficiency (%)
1	0.70	35	300	Original
2	0.64	31	330	91.43
3	0.48	24	360	68.57
4	0.38	19	390	54.29
5	0.28	14	450	40.0

It has also been observed that breakthrough time and uptake capacity at breakpoint is decreased and exhaustion time is increased with each cycle. This may be due to the adverse effect of desorbing agent on the binding sites. The metal uptake is dependent on the desorption process, as prolonged desorption can destroy the binding sites or inadequate time for desorption allow the metal to remain onto the biosorbent. The bed length was also decreasing in successive cycles. It may be due to the dissolution of some soluble constituents during desorption. Shortening of breakthrough time shows the loss of biosorption performance. The breakthrough capacity has been found to be decreased significantly in the fifth cycle in comparison to original capacity showing the deterioration of biosorbent.

4. Conclusions

In this paper, data obtained from batch and column studies has been used to study the adsorption capacity and mechanism involved. Following outcomes have been drawn:

- Involvement of various functional groups (–NH, –CH, –C to N, and –C=C) is indicated by the observed FTIR spectral changes after metal adsorption.
- Adsorption of chromium on algal surface is confirmed by changes in surface morphology observed in SEM.
- Relatively higher adsorption capacity observed for free algal biomass based on Langmuir and Freundlich isotherm shows its greater potential for chromium removal as compared to that for immobilized form.
- Value of separation factor (R_L) for both the biosorbents ranging between 0 and 1 support the favorability of the chromium adsorption.
- Application of data from kinetic studies to Intraparticle diffusion model indicated the involvement of surface sorption for both the biosorbents.
- Temkin, Flory–Huggins and Dubinin–Radushkevich models applied to the equilibrium data inferred that biosorption of chromium by both biosorbents is physisorption and spontaneous process.
- Optimal conditions for maximum adsorption capacity (0.70 mg/g) in column mode, for the present biosorbent are 20 mg/L initial chromium concentration at flow rate of 1 mL/min, and 10 cm bed height.
- Bohart–Adams model applied to the data indicated good agreement between the predicted and experimental values.
- Higher adsorption capacity of this alga as compared to other biosorbents reported in the literature, and good adsorptive capacity after five consecutive sorption–desorption cycles suggests the utility of this biosorbent for chromium removal and further designing and upscaling of the adsorption process.

Acknowledgements

The authors acknowledge financial assistance provided by Guru Jambheshwar University of Science and Technology, Hisar, in the form of University Research Fellowship.

References

[1] S. Klimmer, H.J. Stan, A. Wilke, G. Bunke, R. Buchholz, Comparative analysis of the biosorption of cadmium, lead, nickel, and zinc by algae, Environ. Sci. Technol. 35 (2001) 4283–4288.
[2] K.K. Deepa, M. Sathishkumar, A.R. Binupriya, G.S. Murugesan, K. Swaminathan, S.E. Yun, Sorption of Cr(VI) from dilute solutions and wastewater by live and pretreated biomass of *Aspergillus flavus*, Chemosphere 62 (2006) 833–840.
[3] K. Vijayaraghavan, J. Jagan, K. Palanivelu, M. Velan, Batch and column removal of copper from aqueous solution using a brown marine alga *Turbinaria ornata*, Chem. Eng. J. 106 (2005) 177–184.
[4] Y. Lu, E. Wilkins, Heavy metal removal by caustic-treated yeast immobilized in alginate, in: R. Hinchee, J.L. Means, R.D. Burris (Eds.), Bioremediation of Inorganics, Battelle Press, Columbus, OH, 1995, pp. 117–124.

[5] Z. Zulfadhly, M.D. Mashitah, S. Bhatia, Heavy metals removal in fixed-bed column by the macro fungus *Pycnoporus sanguineus*, Environ. Poll. 112 (2001) 463–470.
[6] Algaebase in Catalogue of life, Annual checklist, 2005, http://www.algaebase.org.
[7] B.D. Kaushik, Laboratory Methods for Blue-green Algae, Associated Publishing Company, New Delhi, 1987, p. 171.
[8] L.S. Clesceri, A.E. Greenberg, R.R. Trussell, Standard Methods for the Examination of Water and Wastewater APHA, AWWA and WPCF, Washington, DC, 1996.
[9] V. Vadivelan, K. Vasanth Kumar, Equilibrium, kinetics, mechanism, and process design for the sorption of methylene blue onto rice husk, J. Colloid Interface Sci. 286 (1) (2005) 90–100.
[10] Q. Sun, L. Yang, The adsorption of basic dyes from aqueous solution on modified peat-resin particle, Water Res. 37 (2003) 1535–1544.
[11] I. Langmuir, The adsorption of gases on plane surface of glass, mica and platinum, J. Am. Chem. Soc. 40 (1918) 1361–1403.
[12] H. Freundlich, W.J. Helle, Ubber die adsorption in Lusungen, J. Am. Chem. Soc. 61 (1939) 2–28.
[13] B. Kiran, A. Kaushik, C.P. Kaushik, Response surface methodological approach for optimizing removal of Cr (VI) from aqueous solution using immobilized cyanobacterium, Chem. Eng. J. 126 (2007) 147–153.
[14] C. Aharoni, M. Ungarish, Kinetics of activated chemisorption. Part 2. Theoretical models, J. Chem. Soc., Faraday Trans. 73 (1977) 456–464.
[15] M. Hosseini, S.F.L. Mertens, M. Ghorbani, M.R. Arshadi, Asymmetrical Schiff bases as inhibitors of mild steel corrosion in sulphuric acid media, Mater. Chem. Phys. 78 (2003) 800–807.
[16] F. Helfferich, Ion-exchange, McGraw Hills, New York, USA, 1962.
[17] M.N. Zafar, R. Nadeem, M.A. Hanif, Biosorption of nickel from protonated rice bran, J. Hazard. Mater. 143 (2007) 478–485.
[18] M. Horsfall Jr., I. Spiff, Equilibrium sorption study of Al^{3+}, Co^{2+} and Ag^{+} in aqueous solutions by fluted pumpkin (Telfairia occidentalis HOOK f) waste biomass, Acta Chim. Slov. 52 (2005) 174–181.
[19] M.M. Dubinin, The potential theory of adsorption of gases and vapors for adsorbents with energetically non-uniform surface, Chem. Rev. 60 (1960) 235–266.
[20] S. Brunauer, P.H. Emmer, E. Teller, Adsorption of gases in multimolecular layers, J. Am. Chem. Soc. 60 (1938) 309–319.
[21] G. Donmez, Z. Aksu, Removal of chromium (VI) from saline wastewaters by *Dunaliella species*, Process. Biochem. 38 (2002) 751–762.
[22] G.C. Donmez, Z. Aksu, A. Ozturk, T. Kutsal, A comparative study on heavy metal biosorption characteristics of some algae, Process. Biochem. 34 (1999) 885–892.
[23] J.R. Cain, D.C. Paschal, C.M. Hayden, Toxicity and bioaccumulation of cadmium in the colonial green alga *Scenedesmus obliquus*, Arch. Environ. Contamin. Toxicol. 9 (1980) 9–16.
[24] R.E. Treybal, Mass Transfer Operations, 3rd ed., McGraw Hill, New York, USA, 1980, pp. 447–522.
[25] R.A. Perry, C.H. Chilton, Chemical Engineering Handbook, Fifth ed., McGraw Hill, New York, USA, 1973, pp. 16–23.
[26] T.R. Muraleedharan, L. Philip, L. Iyenger, C. Venkobachar, Application studies of biosorbent for monazite processing industry effluents, Bioresour. Technol. 49 (1994) 179–186.